

Gold Nanoparticles

International Edition: DOI: 10.1002/anie.201701605
German Edition: DOI: 10.1002/ange.201701605

Water-Soluble N-Heterocyclic Carbene-Protected Gold Nanoparticles: Size-Controlled Synthesis, Stability, and Optical Properties

Kirsi Salorinne, Renee W. Y. Man, Chien-Hung Li, Masayasu Taki, Masakazu Nambo,* and Cathleen M. Crudden*

Abstract: NHC-Au^I complexes were used to prepare stable, water-soluble, NHC-protected gold nanoparticles. The water-soluble, charged nature of the nanoparticles permitted analysis by polyacrylamide gel electrophoresis (PAGE), which showed that the nanoparticles were highly monodisperse, with tunable core diameters between 2.0 and 3.3 nm depending on the synthesis conditions. Temporal, thermal, and chemical stability of the nanoparticles were determined to be high. Treatment with thiols caused etching of the particles after 24 h; however larger plasmonic particles showed greater resistance to thiol treatment. These water-soluble, bio-compatible nanoparticles are promising candidates for use in photoacoustic imaging, with even the smallest nanoparticles giving reliable photoacoustic signals.

Gold nanoparticles are one of the most often employed and most recognizable nanostructures.^[1] With a multitude of catalytic, imaging, drug delivery, and theranostic applications, these species have attracted considerable attention.^[1b] Recent interest in the use of N-heterocyclic carbenes (NHCs) as alternatives to thiols for the functionalization of gold surfaces^[2] is providing new opportunities in this important area of nanochemistry, and there are several examples of the use of these ligands to stabilize gold nanoparticles.^[3,4] However, for any applications in biological systems, solubility in aqueous media and stability under biological conditions are critical.

Thus far, there are very few examples of water-dispersible NHC-stabilized metal nanoparticles.^[4] In 2015, Johnson published a seminal paper describing Au nanoparticles stabilized with polyethylene glycol (PEG)-functionalized NHCs.^[4a] The PEGylated NHC ligand provided high stability in a range of pH and good stability under biologically relevant electrolyte concentrations. With regard to non-noble metal nanoparticles, Chaudret^[4b] described the use of sulfonate-terminated NHC ligands as stabilizing groups for Pt nanoparticles. Ravoo and Glorius have employed water-soluble

NHC-stabilized metal nanoparticles in catalytic reactions, including the use of bidentate hybrid NHC-thioether ligands for water-soluble Pd and Au nanoparticles.^[4c,d] These systems showed good pH stability; however, as they were destined for catalytic rather than biological applications, stability tests in high ionic strength media or to biologically relevant nucleophiles were not reported.

Considering the potential importance of NHCs for nanostructures, the need to access water-soluble and biocompatible structures cannot be overstated. In this regard, we set out to prepare NHC-functionalized nanoparticles decorated with carboxylate groups chosen for their water solubility, pH tunability, and ease of derivatization.

We began by preparing NHC-Au-Cl (**1**), (Figure 1), through reaction of Me₂S-Au-Cl with the carboxylated benzimidazolium triflate in the presence of K₂CO₃ at 60 °C.^[5] Although effective, this method was often complicated by the presence of [(NHC)₂Au]⁺OTf⁻ (**2**).^[6] Considering the ready availability of **2**, we explored its use as a nanoparticle precursor despite the presence of two strong Au-C bonds.^[7] As shown in Figure 1, both starting materials gave rise to stable gold nanostructures.

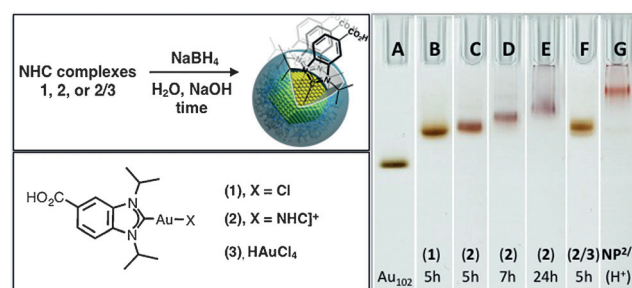


Figure 1. Synthesis of water-soluble NHC-Au nanoparticles by direct reduction of molecular NHC-Au complexes **1** or **2**, or a mixture of **2** and HAuCl₄ (**3**). PAGE (Tris-HCl/glycine) analysis of the purified products. Au₁₀₂ = Au₁₀₂(pMBA)₄₄^[9] as a reference, H⁺ = ripened NPs under acidic conditions.

Reduction of neutral complex **1** with NaBH₄ took place with an immediate color change to dark brown, indicating nanoparticle formation. The carboxylate functionality on the carbene ligand renders the nanoparticles water soluble when deprotonated and makes the surface of the nanoparticles charged, thus the purity and monodispersity of the NHC-Au nanoparticles could be readily analyzed by polyacrylamide gel electrophoresis (PAGE),^[8] which separates species in the gel matrix based on size.

[*] Dr. K. Salorinne, Dr. R. W. Y. Man, Dr. M. Taki, Dr. M. Nambo, Dr. C. M. Crudden
Institute of Transformative Bio-Molecules (WPI-ITbM)
Nagoya University
Furo, Chikusa, Nagoya, 464-8602 (Japan)
E-mail: cruddenc@chem.queensu.ca

Dr. C.-H. Li, Dr. C. M. Crudden
Department of Chemistry, Queen's University
Chernoff Hall, Kingston, Ontario (Canada)

Supporting information and the ORCID identification number(s) for the author(s) of this article can be found under:
<https://doi.org/10.1002/anie.201701605>.

After 5 h reaction time, nanoparticles derived from **1** gave narrow bands in the PAGE gel indicative of high monodispersity (Figure 1, lane B, **NP¹-5h**). A sample of perfectly monodisperse Au₁₀₂(pMBA)₄₄ clusters is included for comparison (lane A, pMBA = *para*-mercaptobenzoic acid).^[9]

Reduction of **2** occurred more slowly, with nanoparticles appearing only after 1 h. NHC-coated nanoparticles displaying a weak surface plasmon resonance (SPR) band at 520 nm were isolated after 5 h (Figure 1, lane C, **NP²-5h**). Based on their behavior on the PAGE gel, nanoparticles produced from **2** after 5 h (**NP²-5h**, lane C) were close in size to those produced from **1** (lane B). Due to the ease of synthesis of **2**, and the similarity of the resulting particles, this method became our preferred choice.

The size of the nanoparticles and the intensity of the SPR band could be controlled by varying the reaction time. Interestingly, the evolution of the NHC-Au nanoparticles to larger sizes proceeded homogeneously, affording NHC-protected gold nanoparticles with narrow size distributions after 7 and 24 h, as evaluated by TEM and gel electrophoresis (Figure 1, lanes D and E, **NP²-7h** and **NP²-24h**; see also the Supporting Information). The bands displayed various colors indicative of the particles being at the edge of the plasmonic regime (ca. 2 nm).^[10]

We also examined the effect of added HAuCl₄ (**3**) as a source of unligated gold for the center of the nanoparticle (see the Supporting Information for experimental details). Using a mixture of **2** and **3** as starting materials, nanoparticles formed much more quickly, with reaction mixtures becoming dark brown immediately. The resulting nanoparticles were similar in size to **NP¹-5h** as determined by PAGE and TEM (Figure 1, lanes B and F). Importantly, both methods lead to nanoparticles with the same NHC: Au ratio within experimental error according to TGA analysis (Sup-

porting Information, Figure S9), and thus only data for **NP^{2/3}-5h** are shown below (see Supporting Information for **NP¹-5h**).

UV/Vis analysis confirmed the presence of plasmonic transitions of varying strength for the different nanoparticles (Figure 2, Table 1). TEM analysis confirmed that nanoparticle cores ranged in size from 2.4 ± 0.3 nm to 3.3 ± 0.4 nm. The smallest NHC-Au nanoparticles, **NP¹-5h** and **NP^{2/3}-5h**, exhibited featureless UV/Vis spectra devoid of an SPR band. These were estimated by TEM to have an average size of 2.0 ± 0.4 nm.

Evidence of NHC binding on the Au nanoparticle surface was afforded by XPS studies, which showed the carbene N 1s peak at about 401 eV (Supporting Information, Figure S10), consistent with our previous studies.^[2b] Furthermore, we observed the binding energy of the alkyl/aromatic carbon at about 285 eV, carboxylate carbon at about 290 eV, and also π to π^* at about 291.5 eV from the C 1s spectrum (Supporting Information, Figure S11).^[11]

The extent of surface functionalization was estimated by TGA analysis. For the larger NHC-Au nanoparticles (**NP²-7h**) with a moderate SPR band, the Au:NHC ratio was determined to be 90:10, whereas smaller nanoparticles (**NP¹-5h** and **NP^{2/3}-5h**) had a ratio of 85:15, both of which correlated well with the respective core sizes based on TEM (Table 1; Supporting Information, Figure S9). Remarkably,

Table 1: Structural properties of NHC-Au nanoparticles.

NP	Core _{TEM} [nm] ^[a]	Au:NHC [%] ^[b]	Au:NHC _{calc} [%] ^[c]	NP _{DLS} [nm] ^[d]	NP _{calc} [nm] ^[c]	SPR [nm] ^[e]
NP^{2/3}-5h	2.0 ± 0.4	85:15	80:20	4.4 ± 1.7	3.8	–
NP²-5h	2.4 ± 0.3	n.d.	n.d.	4.8 ± 1.5	4.3	520
NP²-7h	3.0 ± 0.5	90:10	90:10	8.1 ± 3.0	4.8	525
NP²-24h	3.3 ± 0.4	n.d.	n.d.	n.d.	n.d.	533
NP^{2/3}-H⁺	4.7 ± 0.8	n.d.	n.d.	10.2 ± 4.6	6.1	520

[a] Average diameter of the gold core as determined by TEM. [b] n.d. = not determined. NP metal and ligand content as determined by TGA analysis. [c] Calculated values for metal-to-ligand ratio and hydrodynamic diameter based on TEM core size and surface coverage of NHC ligand^[2b] according to Murray^[12] (see the Supporting Information for details). [d] Average hydrodynamic diameter of NHC-Au NPs in H₂O as determined by DLS, reported as volume distribution. [e] Location of surface plasmon resonance band in H₂O as determined by UV/Vis spectroscopy. Error estimated at ± 0.5 nm.

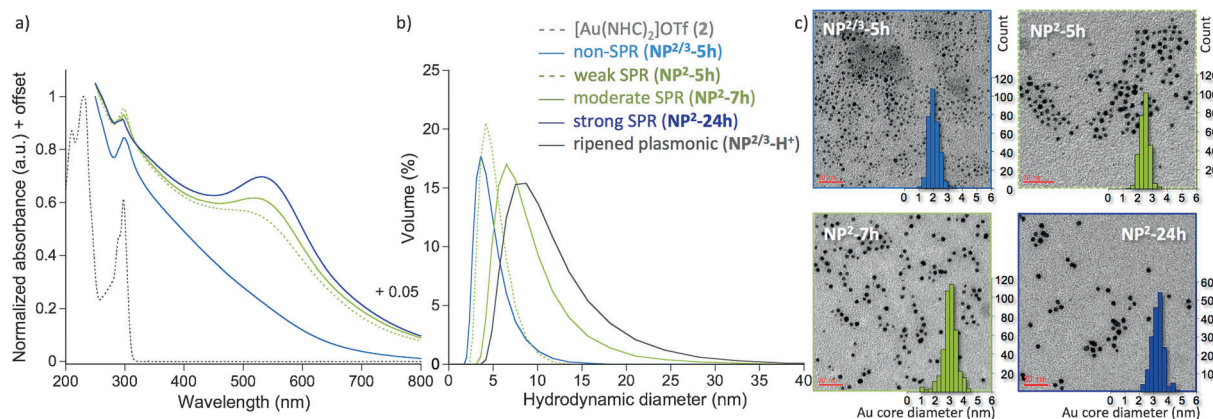


Figure 2. Representative a) UV/Vis spectra, b) DLS volume distribution, and c) TEM images with size histograms of the different sized NHC-Au nanoparticles (see Table 1). UV/Vis and DLS measurements were performed in basic aqueous solutions. For the larger nanoparticles (**NP²-5h**, **NP²-7h**, and **NP²-24h**), SPR resonance is observed at 520–533 nm. Scale bar: 20 nm in all TEM images.

nanoparticles prepared either from neutral complex **1** or a mixture of **2/3**, show almost identical TGA curves, both displaying the same NHC to gold ratio (Supporting Information, Figure S9).

Dynamic light scattering (DLS) studies provided the hydrodynamic size of the nanoparticles including both the gold core and the protecting NHC ligand layer, which affords more accurate assessment of the nanoparticle size in solution (Table 1).^[13] The hydrodynamic diameters in basic aqueous solution were slightly larger than those determined by TEM, but were within error considering the higher standard deviation of the DLS method, particularly with nanoparticles smaller than 5 nm (Figure 2b).^[14]

Having established a robust synthetic route to water-soluble NHC nanoparticles of varying sizes, we then examined their stability in aqueous solution under various conditions. Long-term stability was tested in basic aqueous solutions (pH 8 and pH 10) and monitored by UV/Vis spectroscopy.

Smaller non-SPR nanoparticles (**NP^{2/3}-5h**) were stable up to one month under these conditions, after which time a small SPR band at ca. 520 nm started to appear (Figure 3a). Larger SPR nanoparticles (**NP²-7h**) were stable for at least two months with only small changes in their UV/Vis spectra over that time (Figure 3b). No difference in the stability was observed between pH 8 and 10. Adjusting the pH of the solution to acidic (pH 2) resulted in precipitation of a black solid, which could be redissolved in basic media (pH 10). This pH cycle could be repeated at least five times without any significant changes in the UV/Vis spectra of the non-SPR nanoparticles (**NP^{2/3}-5h**). For the larger nanoparticles (**NP²-7h**), a small sharpening and slight blue-shifting of the SPR band was observed (Supporting Information, Figure S13).^[15]

In protonated form, the NHC-Au nanoparticles are soluble in organic solvents, but have a much shortened lifespan. Within 1–2 days, particles were observed to aggregate and form insoluble solids (MeOH/EtOH/*i*-PrOH) that could not be redissolved. In CH₃CN or DMF, on the other hand, ripening to larger stable plasmonic particles took place (4.7 ± 0.8 nm, **NP^{2/3}-H⁺**), which could be redissolved in water at basic pH and isolated by centrifugal ultrafiltration

(Figure 1, lane G and Figure 3c,d). This is most likely due to hydrogen bonding interactions between the protonated carboxylic acid groups of the neighboring nanoparticles that bring the nanoparticles closer together and facilitate the aggregation^[4c] or ripening processes.

The stability of the NHC-Au nanoparticles in the presence of electrolytes^[16] and biological nucleophiles such as glutathione was also examined. A 150 mM NaCl solution was chosen to simulate physiologically relevant saline concentrations and the stability of the nanoparticles was monitored both by UV/Vis and DLS experiments. Non-SPR nanoparticles (**NP^{2/3}-5h**) were stable for at least 3 days in the electrolyte solution, with a small SPR band starting to emerge at 510 nm after 7 days (Figure 4a). Larger nanoparticles (**NP²-5h**) showed very high stability, with small sharpening of the SPR band after 7 days, suggesting a modest ripening of the particles (Figure 4b). TEM analysis showed that after 7 days, both types of nanoparticles became slightly less monodisperse with the formation of some larger particles in both cases, accounting for approximately 10 % of the particles observed, namely ± 2 % (Supporting Information, Figure S15).

In biological media, glutathione (GSH) is typically found in 0.5–10 mM concentrations;^[17] therefore, NHC-Au nanoparticles ($31 \mu\text{g mL}^{-1}$) were exposed to 2 mM GSH solution under slightly basic conditions (pH 8). This corresponds to a large excess of GSH relative to nanoparticle concentration.^[18] Under these conditions, non-SPR (**NP^{2/3}-5h**) nanoparticles showed low stability and considerable decomposition of the particles to molecular NHC-Au species within 24 h (Supporting Information, Figure S16). Larger SPR nanoparticles (**NP²-5h**) were more resistant to GSH treatment such that a reasonable signal at 515 nm was still present after 24 h.

At higher nanoparticle concentrations (2.2 mg mL^{-1}), under the same conditions, both TEM and PAGE analyses showed etching of the particles, however again the larger SPR (**NP²-5h**) particles still displayed an SPR band even after 5 h of GSH treatment (Supporting Information, Figures S17 and S18).

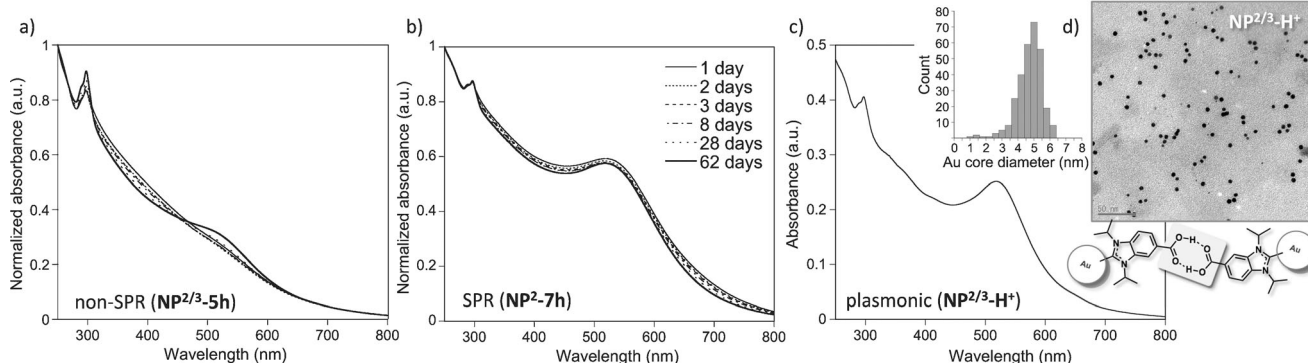


Figure 3. a),b) Long-term stability of NHC-Au nanoparticles in aqueous solution (pH 8) showing UV/Vis spectra of non-SPR (**NP^{2/3}-5h**) and SPR (**NP²-7h**) nanoparticles during 62 days. c),d) Instability of the protonated nanoparticles in organic solvents leads to plasmonic particles (**NP^{2/3}-H⁺**): UV/Vis spectrum in aqueous solution (basic pH) showing an SPR band at 520 nm and TEM image with a size histogram displaying an average size of $4.7(\pm 0.8)$ nm. Scale bar: 50 nm.

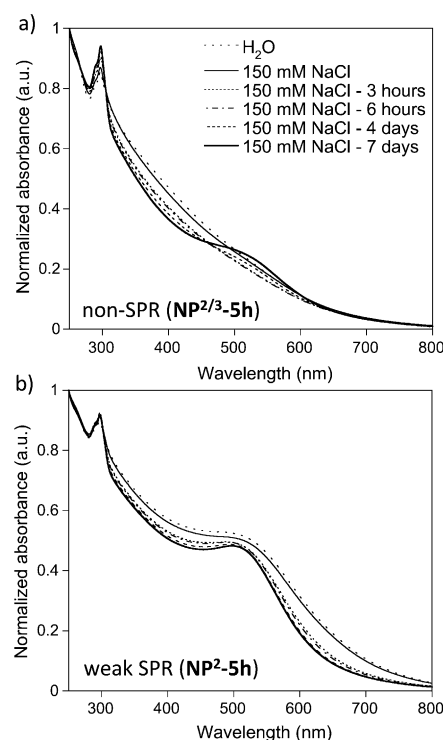


Figure 4. UV/Vis spectra of a) non-SPR (NP^{2/3}-5h) and b) weak SPR (NP²-5h) NHC-Au nanoparticles in aqueous 150 mM NaCl solution at pH 8 over 7 days.

PEG-functionalized NHC-protected Au nanoparticles reported by the Johnson group,^[4a] showed similar long-term stability in aqueous solution, along with susceptibility to etching or aggregation under high electrolyte concentrations or during long exposure to various thiols.^[4a] Thus, the results from this study, in combination with our own, illustrate the effectiveness of the NHC-Au bond at preventing nanoparticle decomposition over time, but the moderate surface density of NHCs on gold may provide space for thiol attack at accessible surface gold atoms.

Finally, we probed the possibility of employing these water-soluble nanoparticles in photoacoustic (PA) imaging, which is an important bio-imaging technique with deep tissue penetration and good spatial resolution.^[19] Irradiating an aqueous solution of nanoparticles with a pulsed laser beam (532 nm) resulted in a reproducible acoustic wave signal (Figure 5). Remarkably, even the smallest nanoparticles (NP²-5h, 2.4 nm), exhibiting only a weak SPR band at 520 nm gave reliable PA signals as shown in Figure 5. The intensity of the PA signal correlated linearly with the concentration of nanoparticles, suggesting that the nanoparticles will be valuable photoacoustic probes.

In conclusion, we have described a bottom-up approach for the synthesis of novel NHC-protected gold nanoparticles employing water-soluble, pH-tunable NHCs. The use of bis NHC or mono NHC-Au complexes as starting materials provided highly monodisperse NHC-protected nanoparticles. Size evolution of the nanoparticles occurred with time with larger particles were still formed with a high degree of monodispersity. The use of H₂AuCl₄ as an additive to promote

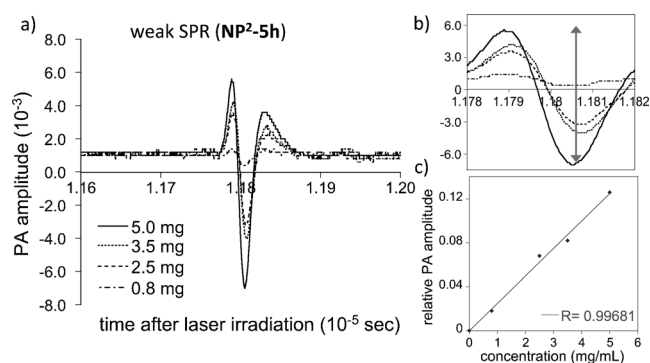


Figure 5. a) Acoustic wave signal detected after irradiating an aqueous solution of weak SPR nanoparticles (NP²-5h) at 532 nm using a pulsed laser beam. b) Zoom-in of the PA signal showing the signal intensity (gray arrow, shown for the most intense signal) that was used to calculate the relative PA amplitude as a function of sample concentration shown in (c).

nanoparticle formation had no effect on the NHC to Au ratio. High temporal stability was observed and reasonable stability to ionic strengths of biological relevance. Instability to thiols continues to be a challenge with these otherwise highly effective ligands, however larger nanoparticles showed resistance to degradation over reasonable time frames for biological applications. The potential for the use of these nanoparticles in photoacoustic imaging was also demonstrated. Further developments of stable nanoparticles and bio-imaging applications are currently underway in our laboratory.

Acknowledgements

JSPS and NU are acknowledged for funding of this research through The World Premier International Research Center Initiative (WPI) program and through a KAKENHI grant (26288023 to C.M.C.). We thank Dr. T. Lahtinen from the University of Jyväskylä for providing Au₁₀₂(pMBA)₄₄. Mr. T. Nemoto and Mr. Y. Uehata (CORNES Technologies Ltd.) are thanked for assistance with measurement of photoacoustic signal. Profs. K. Itami, S. Yamaguchi, and T. Higashiyama are thanked for generous access to their facilities. QU and the Canada Foundation for Innovation are thanked for infrastructure and the Natural Sciences and Engineering Research Council of Canada are thanked for support.

Conflict of interest

The authors declare no conflict of interest.

Keywords: gold nanoparticles · N-heterocyclic carbenes · photoacoustic effect · stability · water solubility

[1] a) R. Jin, C. Zeng, M. Zhou, Y. Chen, *Chem. Rev.* **2016**, *116*, 10346–10413; b) E.-K. Lim, T. Kim, S. Paik, S. Haam, Y.-M.

- Huh, K. Lee, *Chem. Rev.* **2015**, *115*, 327–394; c) S. Eustis, M. A. El-Sayed, *Chem. Soc. Rev.* **2006**, *35*, 209–217; d) M. N. Hopkinson, C. Richter, M. Schedler, F. Glorius, *Nature* **2014**, *510*, 485–496; e) C. Gautier, T. Bürgi, *ChemPhysChem* **2009**, *10*, 483–492; f) S. Knoppe, T. Bürgi, *Acc. Chem. Res.* **2014**, *47*, 1318–1326.
- [2] a) A. V. Zhukhovitskiy, M. J. MacLeod, J. A. Johnson, *Chem. Rev.* **2015**, *115*, 11503–11532; b) C. M. Crudden, et al., *Nat. Chem.* **2014**, *6*, 409–414; c) A. V. Zhukhovitskiy, M. G. Mavros, T. Van Voorhis, J. A. Johnson, *J. Am. Chem. Soc.* **2013**, *135*, 7418–7421; d) C. M. Crudden, et al., *Nat. Commun.* **2016**, *7*, 12654; e) T. Weidner, J. E. Baio, A. Mundstock, C. Grosse, S. Karthäuser, C. Bruhn, U. Siemeling, *Aust. J. Chem.* **2011**, *64*, 1177–1179; f) G. Wang, et al., *Nat. Chem.* **2017**, *9*, 152–156.
- [3] a) S. G. Song, C. Satheeshkumar, J. Park, J. Ahn, T. Premkumar, Y. Lee, C. Song, *Macromolecules* **2014**, *47*, 6566–6571; b) J. Crespo, Y. Guari, A. Ibarra, J. Larionova, T. Lasante, D. Laurencin, J. M. Lopez-de-Luzuriaga, M. Monge, M. E. Olmos, S. Richeter, *Dalton Trans.* **2014**, *43*, 15713–15718; c) M. M. Nigra, A. J. Yeh, A. Okrut, A. G. DiPasquale, S. W. Yeh, A. Solovoyov, A. Katz, *Dalton Trans.* **2013**, *42*, 12762–12771; d) C. J. Serpell, J. Cookson, A. L. Thompson, C. M. Brown, P. D. Beer, *Dalton Trans.* **2013**, *42*, 1385–1393; e) E. C. Hurst, K. Wilson, I. J. Fairlamb, V. Chechik, *New J. Chem.* **2009**, *33*, 1837–1840; f) J. Vignolle, T. D. Tilley, *Chem. Commun.* **2009**, 7230–7232; g) S. Roland, S. Liang, M.-P. Pileni, *Langmuir* **2016**, *32*, 7683–7696; h) M. Rodríguez-Castillo, et al., *Chem. Eur. J.* **2016**, *22*, 10446–10458; see also Ref. [2a].
- [4] a) M. J. MacLeod, J. A. Johnson, *J. Am. Chem. Soc.* **2015**, *137*, 7974–7977; b) E. A. Baquero, S. Tricard, J. C. Flores, E. de Jesús, B. Chaudret, *Angew. Chem. Int. Ed.* **2014**, *53*, 13220–13224; *Angew. Chem.* **2014**, *126*, 13436–13440; c) A. Ferry, K. Schaepe, P. Tegeder, C. Richter, K. M. Chepiga, B. J. Ravoo, F. Glorius, *ACS Catal.* **2015**, *5*, 5414–5420; d) A. Rühling, K. Schaepe, L. Rakers, B. Vönhören, P. Tegeder, B. J. Ravoo, F. Glorius, *Angew. Chem. Int. Ed.* **2016**, *55*, 5856–5860; *Angew. Chem.* **2016**, *128*, 5950–5955.
- [5] A. Collado, A. Gómez-Suárez, A. R. Martin, A. M. Z. Slawin, S. P. Nolan, *Chem. Commun.* **2013**, *49*, 5541–5543.
- [6] R. Jothibasu, H. V. Huynh, L. L. Koh, *J. Organomet. Chem.* **2008**, *693*, 374–380.
- [7] Despite the strength of the metal-carbon bond in NHC metal complexes, cleavage can take place. See for example: C. M. Crudden, D. P. Allen, *Coord. Chem. Rev.* **2004**, *248*, 2247–2273.
- [8] K. Kimura, N. Sugimoto, S. Sato, H. Yao, Y. Negishi, T. Tsukuda, *J. Phys. Chem. C* **2009**, *113*, 14076–14082.
- [9] Au₁₀₂(pMBA)₄₄ was used as a reference compound due to a similar carboxylic acid decorated surface: Y. Levi-Kalishman, P. D. Jadzinsky, N. Kalisman, H. Tsunoyama, T. Tsukuda, D. A. Bushnell, R. D. Kornberg, *J. Am. Chem. Soc.* **2011**, *133*, 2976–2982.
- [10] a) S. Malola, L. Lehtovaara, J. Enkovaara, H. Häkkinen, *ACS Nano* **2013**, *7*, 10263–10270; b) K. Iida, M. Noda, K. Ishimura, K. Nobusada, *J. Phys. Chem. A* **2014**, *118*, 11317–11322.
- [11] a) J. W. Park, J. S. Shumaker-Parry, *ACS Nano* **2015**, *9*, 1665–1682; b) H. J. Lee, A. C. Jamison, Y. Yuan, C. H. Li, S. Rittikulsittichai, I. Rusakova, T. R. Lee, *Langmuir* **2013**, *29*, 10432–10439.
- [12] a) M. J. Hostetler, J. E. Wingate, C. J. Zhong, J. E. Harris, R. W. Vachet, M. R. Clark, J. D. Londono, S. J. Green, J. J. Stokes, G. D. Wignall, G. L. Glish, M. D. Porter, N. D. Evans, R. W. Murray, *Langmuir* **1998**, *14*, 17–30; b) W. P. Wuelfing, S. M. Gross, D. T. Miles, R. W. Murray, *J. Am. Chem. Soc.* **1998**, *120*, 12696–12697.
- [13] Since our NHC-stabilized Au nanoparticles are water soluble only when deprotonated, an additional layer of hydrated sodium cations needs to be accounted for when calculating the hydrodynamic size of the nanoparticles: K. Salorinne, T. Lahtinen, S. Malola, J. Koivisto, H. Häkkinen, *Nanoscale* **2014**, *6*, 7823–7826.
- [14] B. N. Khlebtsov, N. G. Khlebtsov, *Colloid J.* **2011**, *73*, 118–127.
- [15] After each step of the repeated pH cycle, (precipitation and redissolution of the particles), the product is collected by centrifugation. This additionally removes small impurities/insoluble particles that may be present in the solution, which can account for the observed blue-shift.
- [16] a) T. Laaksonen, P. Ahonen, C. Johans, K. Kontturi, *ChemPhysChem* **2006**, *7*, 2143–2149; b) R. Pamies, J. H. Cifre, V. F. Espin, M. Collado Gonzalez, F. G. D. Baños, J. G. de la Torre, *J. Nanopart. Res.* **2014**, *16*, 2376–2387.
- [17] a) G. K. Balendiran, R. Dabur, D. Fraser, *Cell Biochem. Funct.* **2004**, *22*, 343–352; b) P. Maher, *Ageing Res. Rev.* **2005**, *4*, 288–314.
- [18] Based on TGA data, 1 mgmL⁻¹ of NHC-Au nanoparticles contain 1.4 mM (non-SPR, **NP²³-5h**) and 0.8 mM (weak SPR, **NP²-5h**) concentration of NHC ligands in comparison to 2 mM of GSH.
- [19] a) K. Pu, A. J. Shuhendler, J. V. Jokerst, J. Mei, S. G. Gambhir, Z. Bao, J. Rao, *Nat. Nanotechnol.* **2014**, *9*, 233–239; b) L. Nie, X. Chen, *Chem. Soc. Rev.* **2014**, *43*, 7132–7170.

Manuscript received: February 13, 2017

Final Article published: ■ ■ ■ ■ ■ ■ ■ ■ ■ ■

Communications

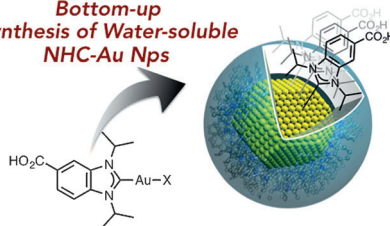


Gold Nanoparticles

K. Salorinne, R. W. Y. Man, C.-H. Li,
M. Taki, M. Nambo,*
C. M. Crudden* ———— ■■■-■■■

Water-Soluble N-Heterocyclic Carbene-
Protected Gold Nanoparticles: Size-
Controlled Synthesis, Stability, and
Optical Properties

Bottom-up
Synthesis of Water-soluble
NHC-Au Nps



Goldwasser: Water-soluble, NHC-functionalized Au nanoparticles (NPs) with tunable core diameters between 2.0 and 3.3 nm were prepared from molecular precursors. Temporal and chemical stability of the NPs were high, with aqueous stability of more than two months. However, exposure to thiols results in etching. All of the NPs tested gave reliable photoacoustic signals that scaled with NP concentration.

